AEIC'95

AL-AZHAR Engineering Fourth
International Conference
December 16-19,1995

المؤتمر العلمى الدولى الرابع
كلية الهندسة - جامعة الأزهر
من ٢٣ إلى ٢٦ رجب ١٤١٦هـ
الموافق١٦ إلى١٩ ديسمبر١٩٩٥م

PHYSICO-CHEMICAL MODELLING OF SHALE-DRILLING FLUID INTERACTION UNDER SIMULATED DOWNHOLE STRESSES

Musaed N. J. AL-Awad[1] and B.G.D. Smart[2]

[1] Petroleum Engineering Department, College of Engineering, King Saud University, P.O. Box 800 Riyadh 11421, Saudi Arabia.

[2] Department of Petroleum Engineering, Heriot-Watt University, Edinburgh, U.K.

ABSTRACT

A mathematical model has been developed for predicting the swelling behaviour of shale when placed in contact with water under moderate pressures and the effect of the swelling on borehole instability. The model is based on thermodynamic theory which suggests that fluid movement into or out of a shale is driven by an imbalance in the partial molar free energy of the shale and the contacting fluid. Conversion of the free energy of each system (fluid and shale) into "total swelling pressure" made it possible to model transient pressures and strains generated in shale. The analytical solution of the radial diffusivity equation is reduced to a simpler form for the model. The model was validated using equipment and experimental techniques which allow continuous monitoring of shale swelling as function of time and distance from the wetting end. It was found that increasing the compaction stress acting on the shale reduced the rate of swelling, and increasing the hydraulic pressure of the fluid on the shale's wetted surface increased the rate of swelling. This behaviour was adequately described by the model which therefore represents a new method for predicting shale swelling as function of time and radial distance under different environments. Swelling strains are then used to predict related changes in shale mechanical properties (failure criteria) and well (in)stability. This model can be used to screen drilling fluids for their ability to control shale swelling, hence minimising the risk of borehole instability.

KEYWORDS

Shale, Swelling, Water Activity, Adsorptive Pressure, Adsorption Isotherm, Drilling Fluids.

INTRODUCTION

On average, drilling problems due to wellbore instability are responsible for about 10 to 20% of the total drilling cost of a well. Further extensive statistical analysis reveals that 80 to 90% of these instabilities occur when drilling through shales [1]. Cost estimates for the industry outside the former Communist countries are in the order of $400-500 millions per year [2]. Problems generally build up in time, starting with fragmentation at the borehole wall,

followed by transfer of the fragments to the annulus and finally culminating in problems such as sticky hole, tight hole, packing off, hole fill, stuck pipe etc. Shale is an argillaceous rock that contains water-sensitive clay minerals. When water (moisture) is adsorbed, the rock swells. Material properties of shale rock under the influence of water have been extensively studied by Chenevert [3-5]. He demonstrated experimentally that the percentage expansion (or strain) of the material is directly proportional to the weight percentage of water adsorbed by the material. Others [6,7] have been studied the effect of moisture change on shale mechanical properties. They found that the change in moisture content is the predominant factor leading to alteration in shale mechanical properties. Hence most compressive wellbore failure problems occur in shales. Those problems can be solved by a combination of chemical and mechanical approaches [8].

Shale Adsorptive Pore Pressure

True stress state of a rock can be expressed by the principal of effective stress. This principal states that, effective stress is equal to total applied stress minus pore pressure. Since the introduction of this principal, a great efforts has been made to measure the pore pressure of rocks so that the true stress state can be determined. For clean, permeable sandstone, it is usually found that the effective stress principal can easily be applied. Direct measurement of the pore pressure is achieved with hydraulic pressure device and the effective stress state thereby computed. However, for fine-grained rocks which contain large amounts of clay (such as shales), pore pressure measurement are usually quite difficult because of the adsorptive forces of the clay platelets, which produce negative internal pressures. No suitable device is known for measuring internal pressures of unsaturated shales; the effective stress approach is therefore not feasible and data are usually presented in another form [4]. As an example, data from compressive strength are presented as a function of rock wetness (moisture content), rather than effective confining pressure. The work of Colback et al [5] is an example of such data. Thus, there have been a need for a better way to express the effective stress of argillaceous rocks. Recently, Chenevert [4] presented a method which can be used to determine adsorptive (negative) pore pressures by direct measurement of aqueous vapour pressure and the application of a basic energy-pressure relationship. He reported adsorptive pressure data as low as -318 MPa. The key of determining the true effective stress of a rock is to determine its true pore pressure. For highly argillecous, compacted rocks such as shales, this is very difficult to do because they exhibit high adsorptive (negative) pore pressure. It may seem remarkable that argillaceous rocks have negative pore pressure which can be calculated using the following formula [4]:

$$P_\pi = \frac{RT}{\overline{V}} \ln \frac{P}{P_o} = \frac{RT}{\overline{V}} \ln a_w \qquad (1)$$

Thus Eq. (1) allows the adsorption pore pressure within the shale to be calculated by the measurement of the relative vapour pressure of the water in equilibrium with the shale. It is not necessary to determine each energy potential acting within the rock, rather than it is necessary to determine only the net equilibrium chemical potential of the entire rock-water mass considered as a unit. Chenevert [4] in his work replaced the relative vapour pressure ratio by the water activity of the system. When the water activity of a shale less than unity, a negative pore pressure exists. The effective normal stress is equal to total normal stress (σ) minus pore pressure, therefore, for calculating the effective stress of argillaceous compacted saturated rocks, we have:

$$\overline{\sigma} = \sigma - \frac{RT}{\overline{V}} \ln a_w \qquad (2)$$

It should be pointed out that if the argillaceous rocks is not compacted and free water exists, then its water activity is equal to unity, and hence the pore pressure is zero, and the effective stress equals total stress. if however, the free water within such rock is pressured then, the standard effective stress equation should be used and pore pressure (P_o) measured with standard devices. In general pore pressure calculations for argillaceous rocks is summarised in Table 1. Colback et al [5] conducted triaxial strength tests on shales and sandstone and showed that for saturated rocks a singular relationship exists between effective confining stress and effective yield strength provided that the internal adsorptive pore pressures of the rock are considered. The hardening effect obtained by drying out the shale is due to the net increase in effective confining stress and probably not due to a decrease in lubrication (it is postulated that water lubricates the rock grains). Figs. 1.a&b shows the usual non-linear response of uniaxial compressive strengths to the wetness of argillaceous rocks. Hence, account must be taken for the water (moisture) content of rock specimens especially for shales, when testing their strength in order to minimise the scatter in rock strength tests carried out at undefined moisture content levels and to facilitate comparison of test data.

MATHEMATICAL MODELLING OF SHALE TOTAL SWELLING PRESSURE

The classical diffusivity equation in its radial form is derived by combining the mass balance equation with Darcy's law. Consider a cylindrical specimen of shale, sealed on all directions except that one facing the wellbore which is exposed to the drilling fluid. The following assumptions are made in order to simplify the derivation [9]:

(i) Homogeneous, isotropic formation.
(ii) Flow is radial and isothermal.
(iii) The drilling fluid filtrate has small and constant compressibility.
(iv) Single phase flow and the shale is fully saturated.

Consider the centre-line of the well as the axis r=0, and the flow of water across the shale thin-walled cylinder of inner radius r and outer radius r+Δr. Then, the Diffusivity Equation in the Radial form will be as follows:

$$\frac{\partial p}{\partial t} = \frac{k}{\mu\ c\ \phi}\left[\ \frac{\partial^2 p}{\partial r^2} + \frac{1}{r}\frac{\partial p}{\partial r}\ \right] \qquad (3.a)$$

Assuming the following boundary conditions are valid:

$$P\Big|_{r=r_w} = P^t_w \qquad 0<t<\infty$$

$$P\Big|_{r=\infty} = CP \qquad 0<t<\infty$$

$$P\Big|_{t=0} = P^t_o \qquad r_w<r<\infty \qquad (3.b, c\&d)$$

and assuming the permeability of the shale to the fluid is constant, this assumption is made in order to simplify the derivation, actually, experiments have shown that permeability of shale varies with swelling and effective stress [10], also, the drilling fluid filtrate viscosity is considered as constant since the flow is isothermal, then the solution of Eq. (7) with the above boundary conditions can be written as follows [11,12] :

$$P_{(r,t)} = P^t_w\left[1 + \frac{2}{\pi}\int_0^\infty e^{-kPU^2}\beta\ \frac{dU}{U}\right] \qquad (4)$$

where,

$$\beta = \frac{J_o(Ur)\ Y_o(Ur_w) - J_o(Ur_w)\ Y_o(Ur)}{Y_o^2(Ur_w)\ J_o^2(Ur_w)}$$

Since it is tedious to integrate Eq. (4), it is approximated with a simpler form. The pressure distribution with a logarithmic scale shows a constant slope for P vs. (r/r_W) up to a certain radius. The constant slope indicates that pressure distribution can be approximated by a logarithmic approximation up to a certain distance as follows [13]:

$$P_{(r,t)} = P_w^t - q \ln r_d \qquad r_d < \xi$$

$$P_{(r,t)} = P_o^t \qquad r_d \geq \xi \qquad \text{(5.a\&b)}$$

$$t_d = \left(\frac{k}{\mu\ c\ \phi}\right) \cdot \left(\frac{t}{r_w^2}\right) = \left(\frac{1}{\lambda}\right) \cdot \left(\frac{t}{r_w^2}\right) \qquad (6)$$

$$\xi = Exp\left(\frac{P_w^t}{q}\right) \qquad (7)$$

$$q = \left[\left(\frac{A3}{\left(\ln t_d + A1\right)}\right) - \left(\frac{A2}{\left(\ln t_d + A1\right)^2}\right)\right] P_w^t \qquad (8)$$

The set of Eqs. (5) to (8) represent the mathematical model which is simulating the interaction between shale and drilling fluid.

EVALUATION OF MODEL PARAMETERS

Total Wellbore Pressure and Total Pore Pressure

Water can move in any direction provided that, the net driving force acting in that direction. Total wellbore pressure is the combination of mud hydraulic and chemical pressures. This total pressure can be calculated using the following expression [5]:

$$P_w^t = P_w + \left(\frac{RT}{\overline{V}} \ln Awm\right) \qquad (9)$$

While the total pore pressure can be calculated using the following expression [5]:

$$P_o^t = K * CP + \left(\frac{RT}{\overline{V}} \ln Aws\right) \qquad (10)$$

Diffusion Coefficient Evaluation

A single diffusion coefficient value is assumed and corrected based on the minimum standard error of estimate. This method is used based on an assumption that, the net change in shale pore structure during swelling process is equal to zero. Thus, a single value is used to predict the total swelling pressure at any given conditions. Although this method is not accurate, it predicts acceptable total swelling pressure values.

EXPERIMENTAL PROCEDURES

Measurement of shale swelling pressure was done by using a specially designed system linked with a data logging system [14]. The rig is consists of the following components as shown in Fig. 2:

(i) A heavy duty compression machines which is able to provide and maintain the necessary axial load during testing. The axial load is measured by using a load cell fitted in the bottom of the triaxial cell.

(ii) A Triaxial Hoek type cell, which is used to accommodate 1.5 inch diameter shale specimens.

(iii) Test fluid reservoir of piston type which is used to inject the test fluid into the sample in the triaxial cell by means of injecting hydraulic oil below the piston which in turn injects the test fluid into test specimen.

(iv) A set of pressure accumulators fitted into the oil-side of the test fluid injection line, and the confining and axial hydraulic lines. These accumulators provides a stabilising effect on the pressure lines which is needed during this study over a long period of time.

(v) A set of linear pressure transducers which provide a continuous measurement of the pressure sets on the system. Also an RDP voltage difference recorder is used in combination with the load cell to measure and record the axial load.

(vi) An interface box which contains a set of full bridge circuits to simulate a reference sample in order to record any change in the strain gauges attached to the test sample.

(vii) An intelligent data logger which provides the required voltage necessary to excite the strains gauges as well as the pressure transducers.

Analysis of Studied Shale

Preserved cylindrical shale samples were cored from bulk material and used through out this study to investigate the mechanisms controlling shale-fluid interaction and its effect on borehole stability. Natural cylindrical core samples (1.5 in. x 2.5 in.) were cored from FMS-Shale bulk samples especially to validate the developed mathematical model. This type of shale was chosen due to its easy coring job and to its reasonable reactivity when contacted with water. Semi-quantitative compositional analysis of this shales was investigated using XRD methods as follows : 13% Illite, 1% Chlorite, 58% Kaolinite, 27% Quartz and Calcite, and 1% Organic Matter.

Drilling (water solutions) Fluids Used in this Study

Test fluids used during the verification of the swelling model were formulated using distilled water and some salts such as Potassium Chloride and Sodium Chloride. These salts are commonly used as a drilling fluid additives. Water activities of the formulated solutions were derived by applying the adsorption method.

Tests Conducted Under Zero Compaction Stresses

In this test, swelling micro-strains were measured under atmospheric conditions. Two strain gauges were attached in two opposed directions one inch far from the specimen (2.5 in. x 1.5 in.) face exposed to the test fluid. Strain gauged samples were coated by a waxy material except one side which is then exposed to test fluid. The sample was then placed in a cell and the test fluid was added. The generated swelling strains were recorded continuously until equilibrium was reached or the required period was covered. Three tests were conducted under the boundary conditions shown in Table 2.

Tests Conducted Under Moderate Compaction Stresses

In this test swelling micro-strains were measured under moderate confining pressures (between 6.89 MPa and 10.35 MPa). Strain gauged samples were coated by a waxy material except the side exposed to the test fluid. Two strain gauges were attached in two opposed places 1 inch far from the specimen (2.5 in. x 1.5 in.) face exposed to the test fluid. The sample was then placed in the triaxial cell and loaded to the provided system and the required axial load and confining pressure were applied. Test fluid was then injected into the cell and the swelling strains as well as the axial, confining and test fluid injection pressures were continuously recorded until equilibrium was reached or the required period was covered. Five tests were conducted under boundary conditions shown in Table 3.

Shale Adsorption Isotherm

Adsorption isotherm relates the amount of clay in a shale to its moisture content. A range of water activities (relative humudities) can be achieved by using a number of vacuum desiccators containing saturated salt solution in their shallow base. Every salt solution provides known relative humidity. Shale samples when placed inside one of these vacuum desiccators, will either gain or lose moisture. The adsorption isotherm then established by plotting moisture content (gained) percent at equilibrium versus salt water activity. Fig. 3 shows the adsorption isotherm of FMS-shale tested in this study.

Swelling Strains -Moisture Content Relationship

When shale moisture content is altered, its dimensions may change due to this alteration. This change in sample dimensions in turn produces swelling strains in that sample. Each cylindrical shale specimen was attached with two strain gauges in order to measure any change in sample dimensions in both directions normal and parallel to bedding planes. The strain gauged sample was then placed in a high relative humidity desiccator, and the swelling strains in both direction were recorded using the data logging system. When the sample was placed in the desired desiccator, strain gauges leads were connected to the interface box, then to the data logger, after that, the desiccator was evacuated using vacuum pump. Sample weight is measured at specified time intervals by opening the desiccator and weighing the sample using electronic balance. When there was no change in sample weight, test was terminated. Fig. 4 represents the relationship between moisture content and swelling strains for FMS-shale obtained by averaging the results of three experimental runs.

EXPERIMENTAL RESULTS MODELLING AND DISCUSSION

Total swelling pressure can be predicted by applying the developed mathematical model. Shale specimens were conditioned in a vacuum desiccators containing saturated salt solution, then were mounted into the test arrangement. Test total wellbore pressure was calculated using Eq. (5) while shale total pore pressure was calculated using Eq. (6). The recorded voltages from the installed pressure transducers and voltages recorded by strain gauges attached to the sample were converted to pressures and strains respectively using calibration curves.

Calculation of Experimental Total Swelling Pressure

The resulting data obtained from experimental programme were arranged on the form of relationships between time and swelling strains. The recorded swelling strains were transformed to moisture content using the relationship between moisture content and swelling strains established earlier for FMS-Shale (Fig. 4). Then the transformed moisture contents were converted to water activities using the adsorption isotherms established for FMS-Shale (Fig. 3). The obtained water activities then were inserted into the thermodynamic relationship shown in Eq. (1) and experimental total swelling pressure was calculated.

Figs. 5 to 8 representing the experimental total swelling pressure for FMS-Shale generated under various boundary conditions and calculated using the above procedure.

Assumption of Wellbore Radius

Tests conducted herein using the designed rig were efficiently simulates the real shale-drilling fluid interaction which occurs in the wellbore. However, this test does not account for the wellbore radius as the model does. Wellbore radius is an integral part of the mathematical model as shown in Eq. (6). This effect is clearly come into view when plotting the wellbore radius against the relative position of the stain gauge to the borehole as shown in Fig. 9. Hence to avoid this problem, the wellbore radius was assumed to be variable and the predicted results were made for various wellbore radii ranging from 1 to 5.5 inches. Thus this model can predict total swelling pressure for any desired wellbore radius and the same experimental data can be used in all these predictions.

Evaluation of Model Constants

The developed model is function of several parameters which must be evaluated in order to predict total swelling pressure of shales. These parameters are A1, A2, A3, and diffusion coefficient. The evaluation of these constants is summarised in the following steps:
(i) Assume a starting value for the wellbore radius.
(ii) Substitute the assumed wellbore radius and test boundary conditions including total wellbore pressure and shale total pore pressure into Eq. (5).
(iii) Assume a starting values for A1, A2, A3 and diffusion coefficient.
(iv) Calculate theoretical total swelling pressure and find the standard error of estimation between experimental and theoretical pressures data points.
(v) Change the assumed values in step (iii) until minimum standard error is found, hence, the values assumed in step (iii) are considered as the model constants for the assumed wellbore radius.
(vi) Assume another value for the wellbore radius and repeat the above steps, keeping A1, A2 and A3 values constants while changing diffusion coefficient value until minimum error of estimation is found.

Evaluation of Diffusion Coefficient

Because it tedious to evaluate the parameters composing the diffusion coefficient term which include, sample permeability, porosity, and compressibility while testing, they were combined together in one term and defined as the diffusion coefficient. This coefficient is mathematically expressed as follows:

$$\lambda = \left(\frac{\mu c \phi}{k} \right) \tag{11}$$

The value of this coefficient was evaluated by trial and error method in which the difference between the experimental and theoretical total swelling pressure was minimum.

Evaluation of the Theoretical Total Swelling Pressure

The Theoretical total swelling pressure can be evaluated for any given conditions by applying the following steps:
(a) when constant value diffusion coefficient is assumed, model constants and the diffusion coefficient values are estimated for the required wellbore radius from the established relationships. Then, the total swelling pressure can be calculated for any required conditions.

(b) when variable diffusion coefficient is assumed, the model constants A1, A2, and A3 are estimated based on the assumed wellbore radius. The relationship between diffusion coefficient and time and the other parameters mentioned above are substituted into the mathematical model represented by Eqs. 5 to 8, then, total swelling pressure is estimated for any required boundary conditions. Figs. 10.a&b show the predicted total swelling pressure using both methods. It is clear that the variable diffusion coefficient method predicted more precise data than the constant value method. It must be noticed that for any assumed wellbore radius the corresponding set of model constants can predict a theoretical total swelling pressure with good agreement with the experimental data as shown in Figs. 11 to 14.

Measurement of Moisture Advancement

In order to investigate the accuracy of the developed model, all the three samples which was tested under atmospheric conditions were cut into five sections after the termination of the test period. Moisture content at each section was determined by placing the sample inside an oven at 105°C until constant weight was reached, and then the moisture content was calculated and converted to water activities using the adsorption isotherm curve established earlier as shown in Fig. 15. The results herein represents a good agreement between the predicted and measured water activities during testing period. Due to the difficulties in extracting the samples from the rubber sleeve after the termination of test conducted at moderate confining pressures, this process was not evaluated.

Comparison Between Experimental and Theoretically Predicted Results

Predicted total swelling pressure values are very sensitive to model constants A1, A2, A3, and diffusion coefficient. Thus, predicted data when using constant value diffusion coefficient has less accuracy. This standard error was minimised when variable diffusion coefficient method was applied. This model is able to predict shale total swelling pressure if the boundary conditions are estimated accurately and the model constants are evaluated precisely. The results obtained in this study showed that, controlling water activity of drilling fluids is of great importance for hole stability. Fig. 16 shows how the swelling pressure is reduced by three times when the drilling fluid activity is reduced from 0.9 to 0.85. This can be accomplished by adding more salts to the drilling fluid. Fig. 17 shows the effect of compaction pressure (combination of axial and confining stresses) in controlling fluid movement into the test samples, which is in turn decreased the rate of swelling generation. Wellbore pressure also plays an important role in maintaining hole stability when drilling argillaceous formations. When wellbore hydraulic pressure is increased the magnitude of the swelling pressure is increased as shown in Fig. 18. It should be recognised that, the reduction of wellbore hydraulic pressure can minimise swelling process but in the other hand it may affect the hole stability by removing the support given to the sides of the wellbore which may lead to wellbore collapse. To solve this problem, drilling fluids composition must be controlled such that a suitable material may added to plug shale pore and micro-fractures presented initially in the shale. This can minimize the fluid invasion into the shale formation and at the same time provides the required support to the wellbore sides and prevents the occurrence of borehole collapse.

The Significance of Shale Swelling on Borehole Stability

It is well known that when shale is brought into contact with drilling fluids it swell and lose a great portion of its strength depending on the magnitude of swelling pressure generated in that shale. In order to characterise this fact, the classical Mohr-Coulomb failure criteria was modified to account for the total swelling pressure term. This was made because shale swelling is the same as pore pressure, it effects in all directions. Based on the effective stress principal, the total swelling pressure has the same mechanism in unsaturated shales. Mohr-Coulomb failure criteria in combination with shale total swelling pressure were used to predict the reduction in shale strength when brought in contact with drilling fluids.

Fig. 19 shows the predicted failure envelope based on the experimental data obtained by applying the total swelling pressure concept. The change in uniaxial compressive strength was calculated using data obtained from swelling tests. It is found that FMS-Shale uniaxial strength was impacted by the increases in water content as shown in Fig. 20. This result is in complete agreement with the results obtained by Chenevert [4] and Colback [5] which are shown in Fig. 1.

CONCLUSIONS AND RECOMMENDATIONS

1. The present model includes the chemical properties of the mud and shale into the calculation of moisture induced strain. It is therefore more convenient to apply in the practical applications.

2. Knowing the moisture induced strains which are then converted into a swelling pressure values, the stress distribution around the wellbore can be calculated by the application of the proper failure criterion.

3. This model related the chemical forces in both shale and drilling fluid to the confining pressure which can provide a useful information when designning drilling fluids which minimizes wellbore instability.

4. The adsorption isotherm test is an excellent way to determine the reactive potential of a shale. It provides the net effect of all clays and ions present from a hydration point view.

5. Tested shales were found to react chemically with distilled water, which is an indication that shales which do not contain smectite can indeed cause hole problems after a long time of exposure.

6. It is recommended to perform a similar work to study the effect of capillary pressure and system (rock-fluid) wettability on the mechanism of fluid invasion through shales and on the overall stability of argillaceous formations.

7. The mathematical model developed to predict shale swelling pressure under elevated stresses need to be modified to account for temperature, and variable overburden stress as well for unequal horizontal stresses. More experimental work is needed to include different types of reactive shale as well as various types of drilling fluid components.

5. The diffusion coefficient is function of several parameters, including, test (invading) fluid viscosity and compressibility, rock permeability, porosity and compressibility. Hence further studies is recommended to asses evaluation methods of the above parameters under realistic stresses enabling the estimation of diffusivity coefficient parameters at laboratory.

REFERENCES

[1] Santarelli, F.J. , Chenevert, M.E., and Osisanya, S.O. :"On the Stability of Shales and Its Consequences in terms of Swelling and Wellbore Stability," Paper no. 23886 on the IADC/SPE Drilling conference, New Orleans, Louisiana, Feb. 18 - 21, 1992.

[2] Bol, G.M. and Sau-Wai Wong : "Borehole Stability in Shales, "SPE 24975, European Petroleum Conference, Cannes, France, Nov. 16 - 18, 1992.

[3] Chenevert, M.E. :"Shale Alteration by Water Adsorption," JPT, Sept. 1970, pp114-1148.

[4] Chenevert, M.E. : "Adsorptive Pore Pressure in Argillaceous Rocks," Proc., 11th Symposium on rock Mechanics, U. of California, Berkeley, June 16 - 19, 1969.

[5] Chenevert, M.E. and Osisanya, S.O. : "Shale Swelling at Elevated Temperature and Pressure," 33rd. US Symp. on Rock Mechanics, New Mexico, June 3-5, 1992, pp869-878, 1992.

[6] Colback, P.S..B. and Wiid, B.L. : " The Influence of Moisture Content on the Compressive Strength of Rock," Proc. of 3rd. Canadian Sump. on Rock Mech. Toronto, 1975.

[7] Hall, A.H. and Mody, F.K. : "Experimental Investigation of the Influence of Chemical Potential on Wellbore Stability," Paper no. 23885 on the IADC/SPE Drilling Conference, New Orleans, Louisiana, Feb. 18 - 21, 1992.

[8] Steiger, R.P.: "Advanced Triaxial Swelling Tests on Preserved Shale cores," Int. J. Rock Mech. Sci. & Geomech. Abstr. vol. 30 No.7, 1993, pp 681-685.

[9] Matthews, C.S. and Russell, D.G. : "Pressure Build-up and Flow Tests in Wells," SPE Monograph, Volume 1, p4-7, 1967.

[10] Chenevert, M.E. and Sharma, A.K. : "Permeability and Effective Pressure of Shales," SPE 21918, 1991.

[11] Carslaw, H.S. and Jaegar, J.S. : "Conduction of Heat in Solids," 2nd. ed., London, Oxford University Press, 1959.

[12] White, P.W., and Moss, J.T.: "Thermal Recovery Methods," Pennwell Books Publishing Co., Tulsa, Oklahoma.

[13] Morita, N., Black, A.D. and Fuh, G.F. : "Theory of Lost Circulation Pressure," SPE 20409, 1990.

[14] Musaed N. J. Al-Awad : "Physico-Chemical Modelling of Shale-Drilling Fluid Interaction and its Application to Borehole Stability Studies.", Ph.D. Thesis, Department of Petroleum Engineering, Heriot-Watt University, Edinburgh, U.K., September, 1994.

NOMENCLATURE

a_w	= Water activity.
Aws	= Shale water activity.
Awm	= Mud water activity.
A1, A2 & A3	= Testing constants appears in Eq. (8).
B(T)	= Constant for a given substance at a given temperature.
c	= Total compressibility.
CP	= Confining pressure.
FMS	= Friable Mudstone.
$\bar{f}_i$	= Fugacity.
k	= Formation permeability.
K	= Constnat appears in Eq. (10).
P_w^t	= The total wellbore pressure.
P_o^t	= The total pore pressure.
P_W	= Wellbore (Mud) hydraulic pressure.

P_o = Pore fluid pressure.

P_π = Swelling Pressure.

q = Pore pressure gradient approximation.

R = Gas constant.

r = Radial distance from well centre.

r_d = Dimensionless radius, r/r_w.

r_w = Wellbore radius.

T = Absolute temperature.

t = Exposure time.

t_d = Dimensionless time.

u_i = Chemical potential of a system.

U = Constant appears in Eq. (4).

$\overline{V}$ = Pure water partial pressure.

β = Constant appears in Eq. (4).

$\overline{\sigma}$ = Effective normal stress.

σ = Total normal stress.

λ = Diffusion coefficient.

μ = Drilling fluid filtrate viscosity.

ϕ = Porosity.

Table (1) General Analysis of Pore Pressure in Argillaceous Sediments.

Case	Pore Pressure Equation	Measurement Method
Compacted, saturated Argillaceous rock with no free water.	$\bar{\sigma} = \sigma - P_{\pi}$	$\bar{\sigma} = \sigma - \frac{RT}{\bar{v}} \times \ln(a_w)$ $P_o = 0$
Uncompacted, saturated Argillaceous rock with free water in drained conditions.	$\bar{\sigma} = \sigma$	$P_{\pi} = 0$ and $P_o = 0$
Uncompacted, saturated Argillaceous rock with free water in undrained conditions.	$\bar{\sigma} = \sigma - P_o$	$P_{\pi} = 0$ and $P_o > 0$ and measured with standard devices.

Table (2) Boundary Conditions of Tests Conducted Under Ambient Confinement.

[1]	[2]	[3]	[4]	[5]	[6]	[7] = [5] - [6]	[8] = [6] - [6]	[9]
Test no.	Aws	Awm	CP=P_w (MPa)	P^t_w (MPa)	P^t_o (MPa)	CP^t_w (MPa)	CP^t_o (MPa)	Axial Load (kN)
1	0.80	.85	0.0	-22.64	-31.10	8.44	0.0	0.0
2	0.80	.90	0.0	-14.67	-31.10	16.40	0.0	0.0
3	0.80	1.0	0.0	0.0	-31.10	31.10	0.0	0.0

Test-1. = 30.5% by weight NaCl. Test-2. = 24% by weight KCl.
Test-3. = Distilled Water.

Table (3) Boundary Conditions of Tests Conducted Under Moderate Confinement.

[1]	[2]	[3]	[4]	[5]	[6]	[7]	[8] = [6] -[7]	[9] = [7] -[7]	[10]
Test no.	Aws	Awm	CP (MPa)	P_w (MPa)	P^t_w (MPa)	P^t_o (MPa)	CP^t_w (MPa)	CP^t_o (MPa)	Axial Load (kN)
4	0.85	0.95	10.34	3.45	-3.70	-12.29	8.60	0.0	11.78
5	0.85	0.95	8.620	3.45	-3.70	-14.02	10.32	0.0	9.81
6	0.85	0.95	6.895	3.45	-3.70	-15.74	12.05	0.0	7.85
7	0.85	0.95	6.895	1.72	-5.42	-15.74	10.32	0.0	7.85
8	0.85	0.95	6.895	5.17	-1.97	-15.74	13.77	0.0	7.85

Test-4. = 12% KCl by weight. Test-5. = 12% KCl by weight.
Test-6. = 12% KCl by weight. Test-7. = 12% KCl by weight.
Test-8. = 12% KCl by weight.

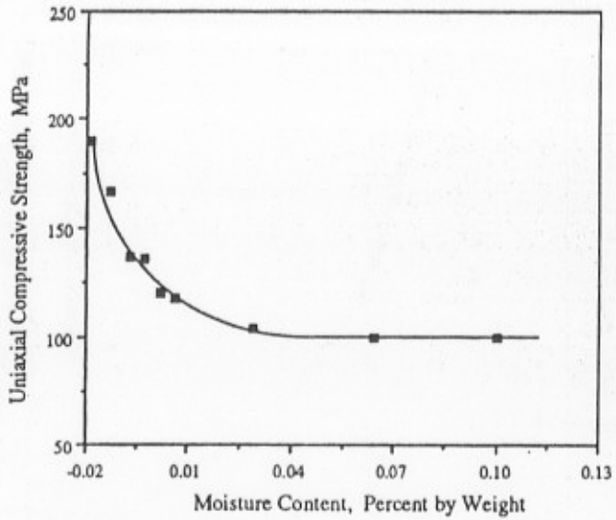

Fig. 1.a : Relationship between Uniaxial Compressive Strength and Moisture Content for Quartzitic Shale, data from Colback et al [ref. #6].

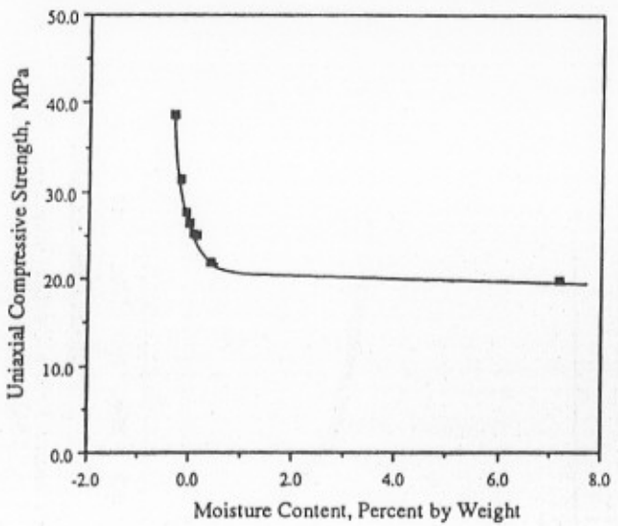

Fig. 1.b : Relationship between Uniaxial Compressive Strength and Moisture Content for Quartzitic Sandstone, data from Colback et al [ref. #6].

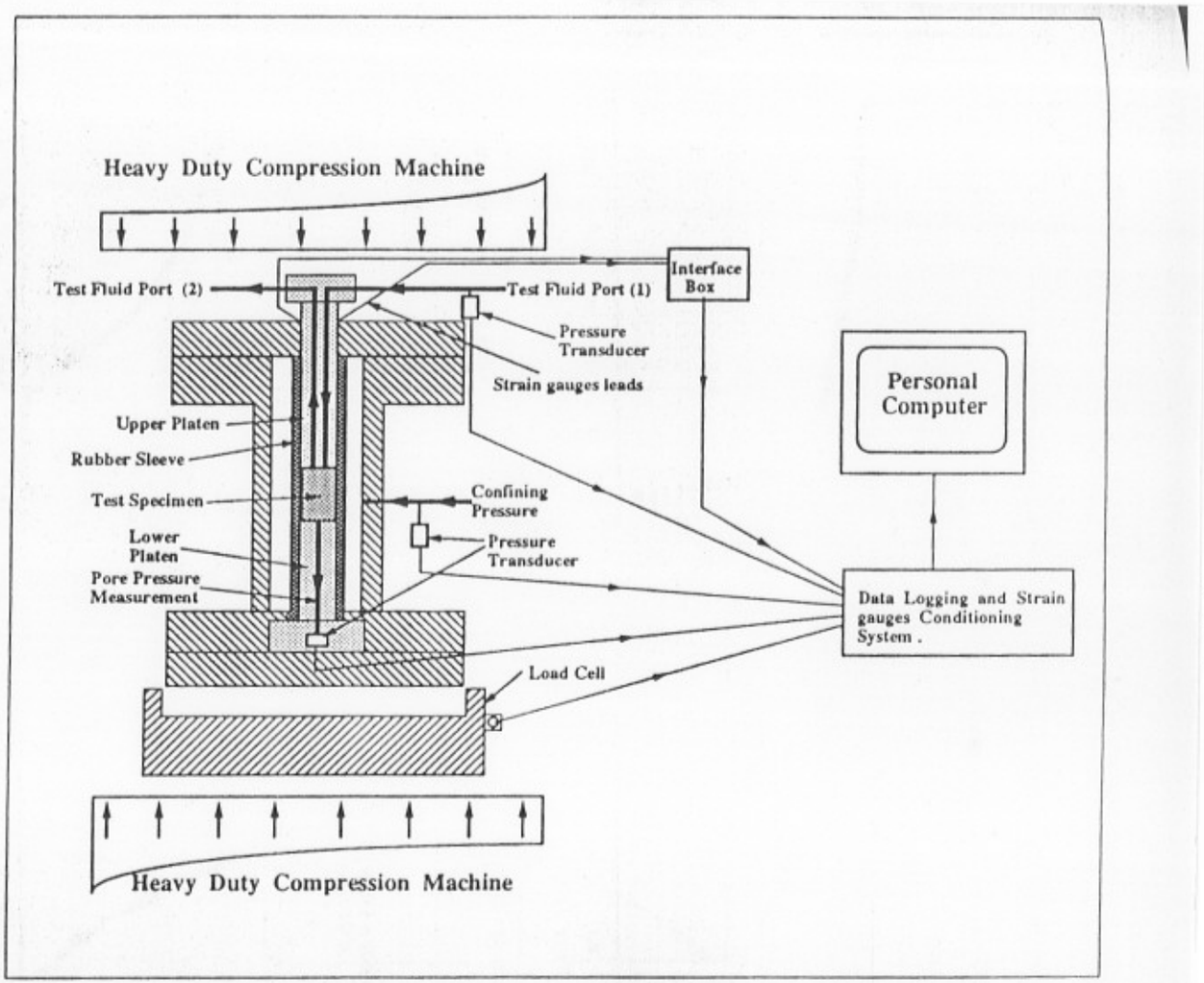

Fig. 2 : Schematic Diagram of the Triaxial Cell and Data Logging System.

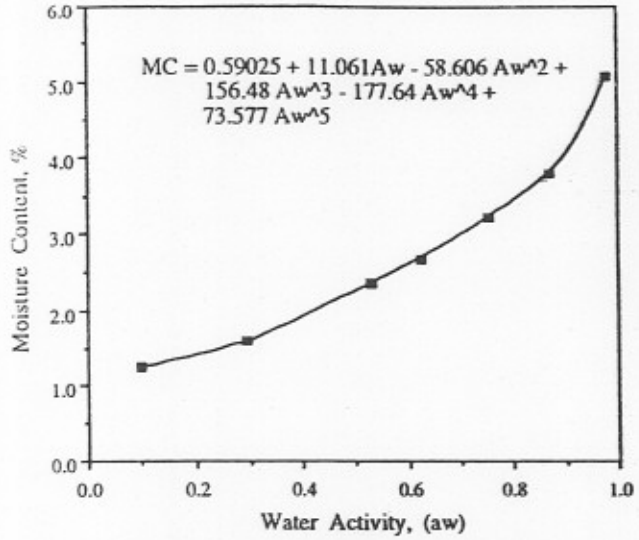

Fig.3 : Moisture Content-Water Activity Relationship (Adsorption Isotherm) of FMS-Shale.

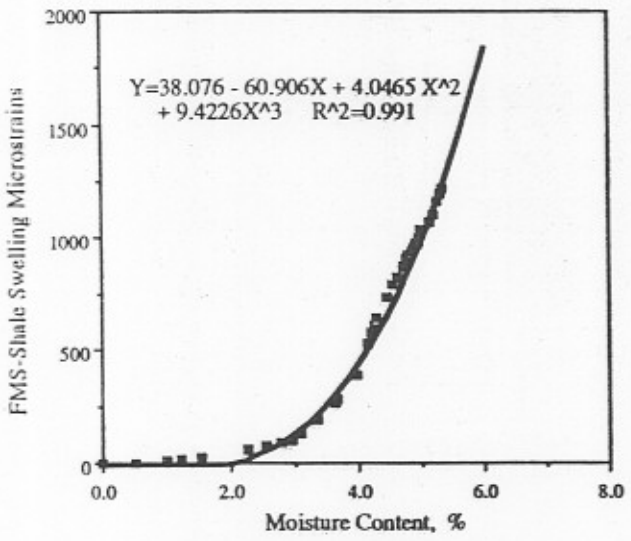

Fig. 4 : Relationship Between Moisture Content and Swelling Microstrains for FMS-Shale.

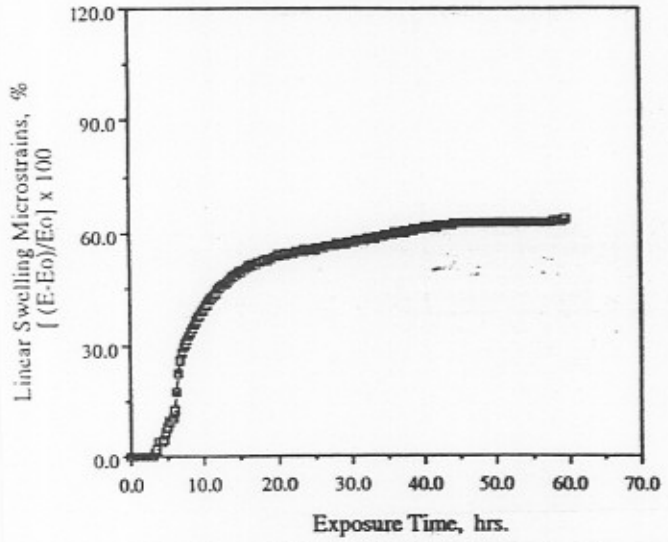

Fig. 5 : Experimental Vertical Swelling Microstrains Generated in FMS-Shale Uder Test #1 Conditions.

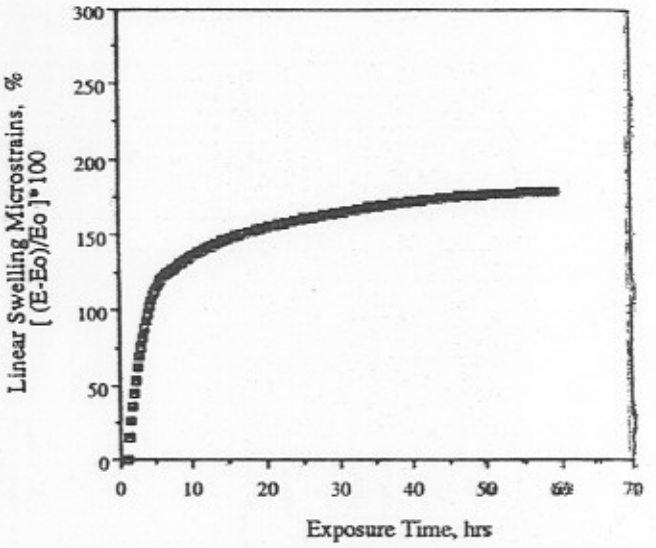

Fig. 6 : Experimental Vertical Swelling Microstrains Generated in FMS-Shale Under Test #3 Conditions.

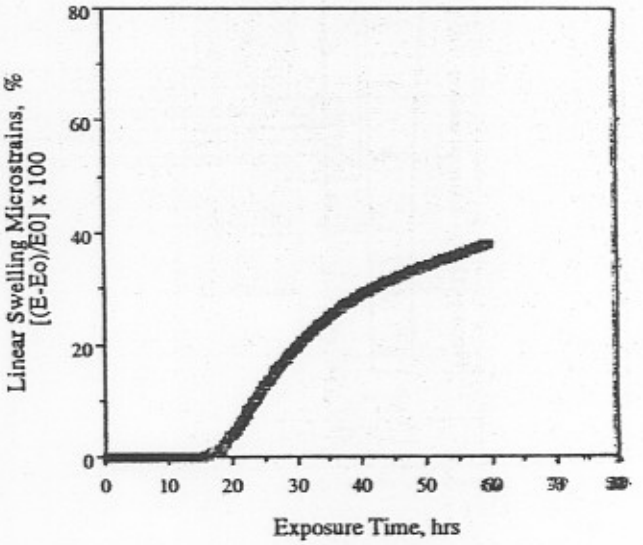

Fig. 7 : Experimental Vertical Swelling Microstrains Generated in FMS-Shale Under Test #5 Conditions.

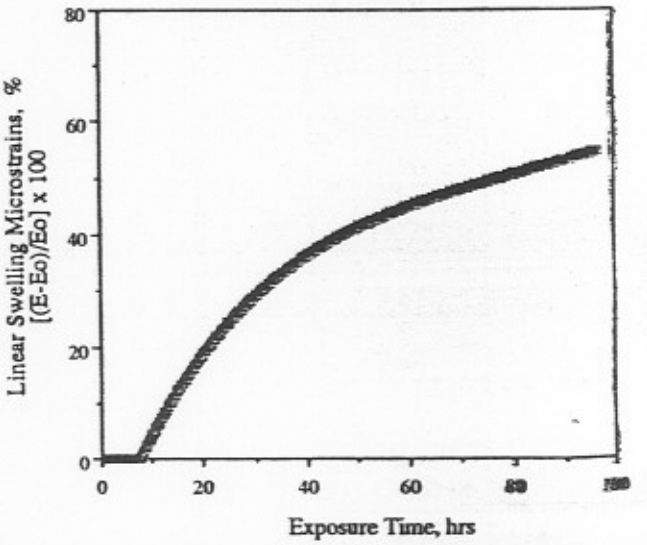

Fig. 8 : Experimental Vertical Swelling Microstrains Generated in FMS-Shale Under Test #8 Conditions.

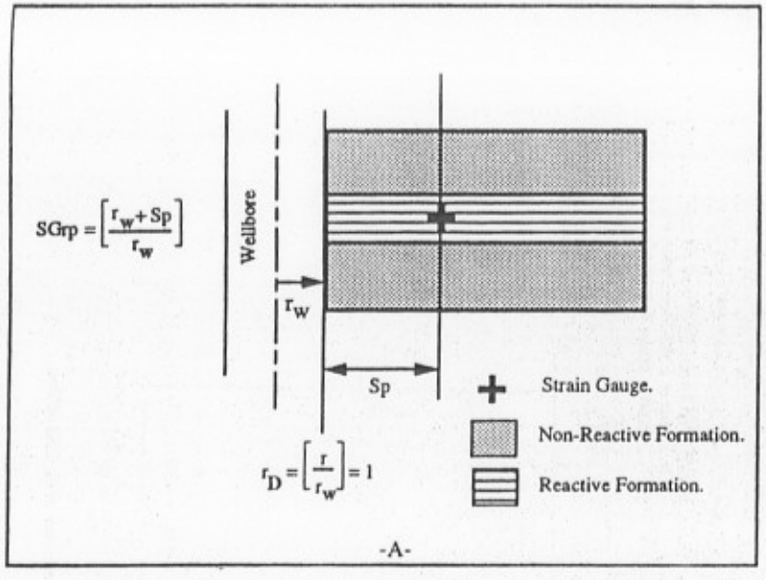

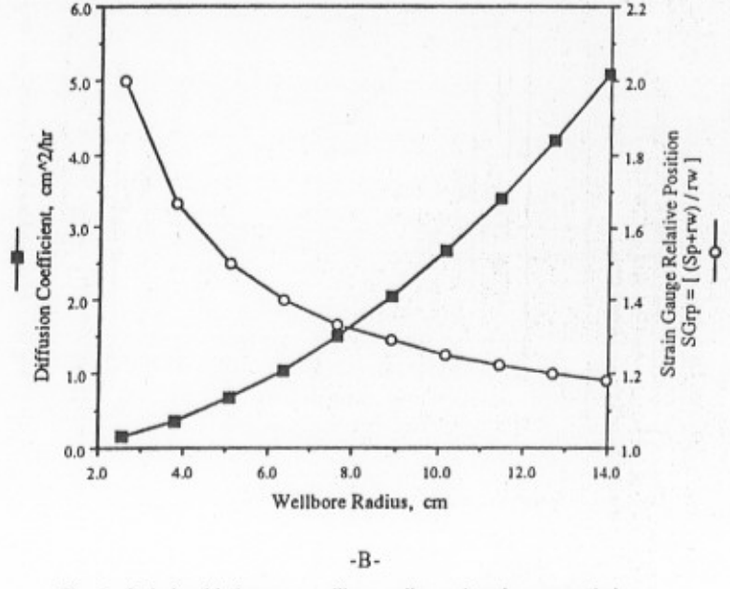

Fig. 9 : Relationship between wellbore radius and strain gauge relative position and their effect on diffusion rate coefficient (Test -1-).

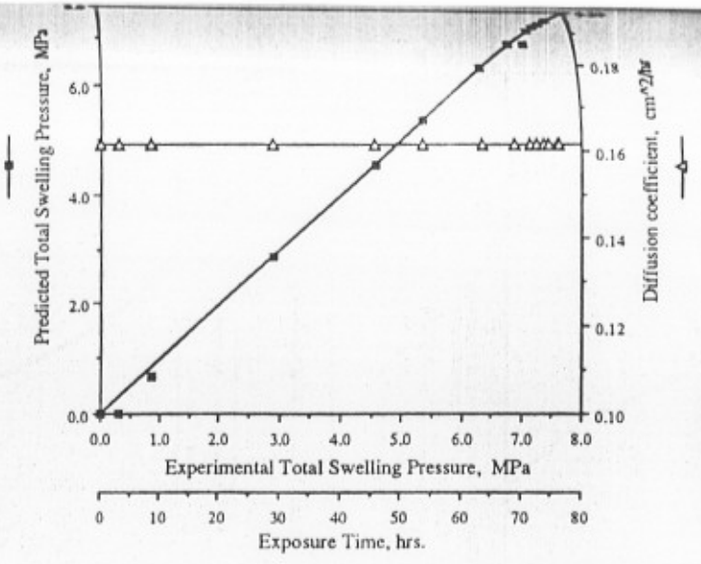

Fig. 10.a : Predicted Total Swelling Pressure for FMS-Shale Using Constant Diffusion Coefficient Method at (r/rw) = 2 and Data of Test #1.

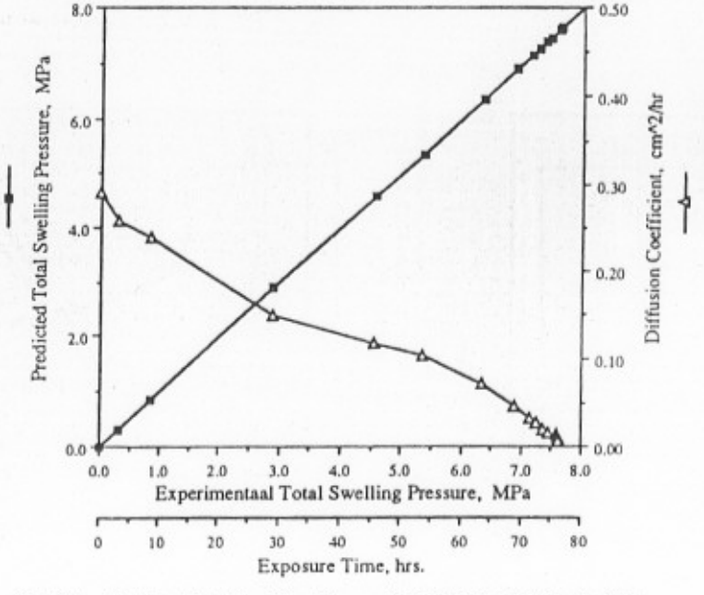

Fig. 10.b : Predicted Total Swelling Pressure for FMS-Shale Using Variable Diffusion Coefficient Method at (r/rw) = 2 and Data of Test #1.

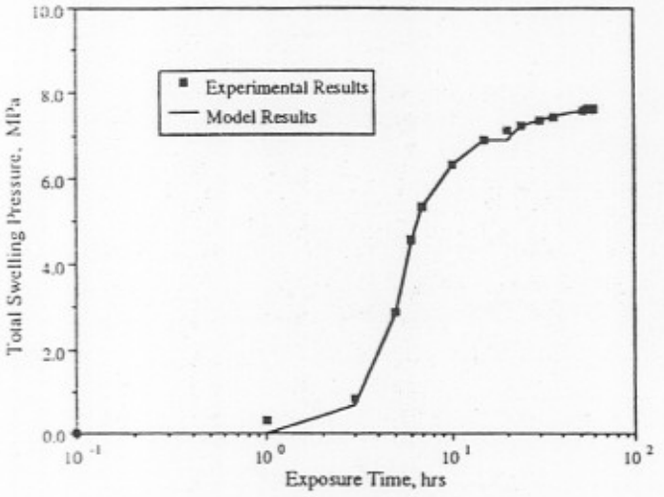

Fig. 11 : Comparison between Experimental and Theoretical Total Swelling Generated in FMS-Shale when Exposed to 30.5% NaCl Solution under Test -1- Conditions.

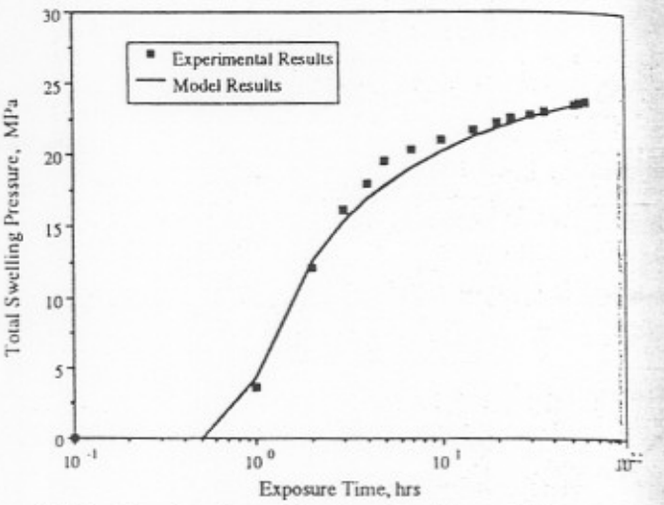

Fig. 12 : Comparison between Experimental and Theoretical Total Swelling Generated in FMS-Shale when Exposed to Distilled Water under Test -3- Conditions.

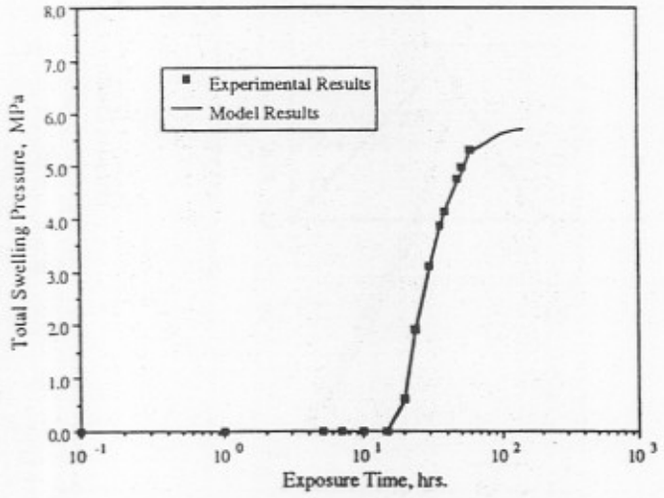

Fig. 13 : Comparison between Experimental and Theoretical Total Swelling Generated in FMS-Shale when Exposed to 12% KCl Solution under Test -5- Conditions.

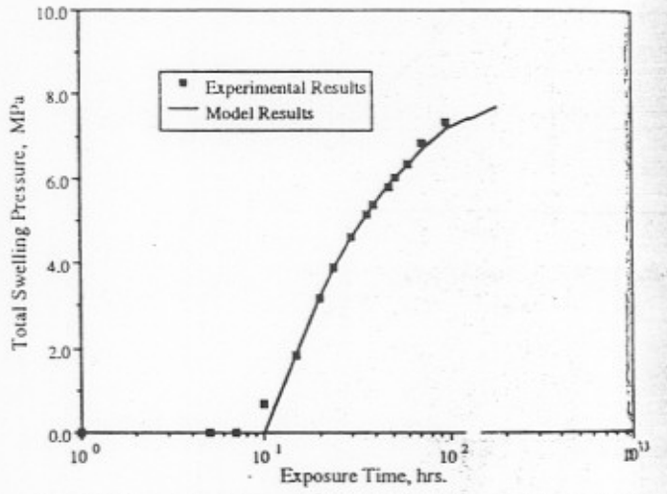

Fig. 14 : Comparison between Experimental and Theoretical Total Swelling Generated in FMS-Shale when Exposed to 12% KCl Solution under Test -8- Conditions.

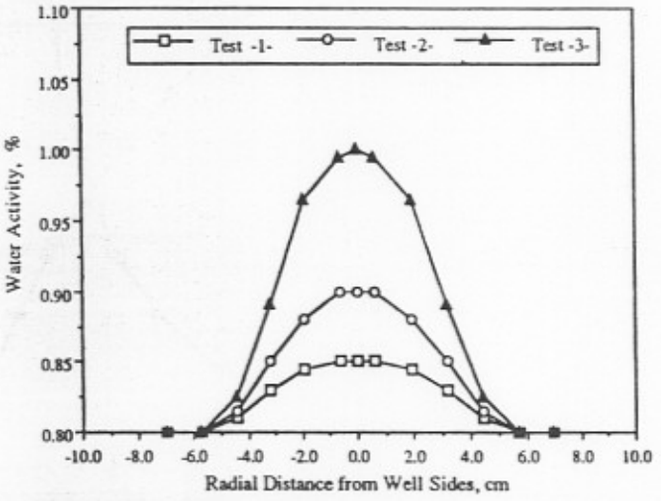

Fig. 15 : Measured Moisture Content on Test Specimens at the End of Test.

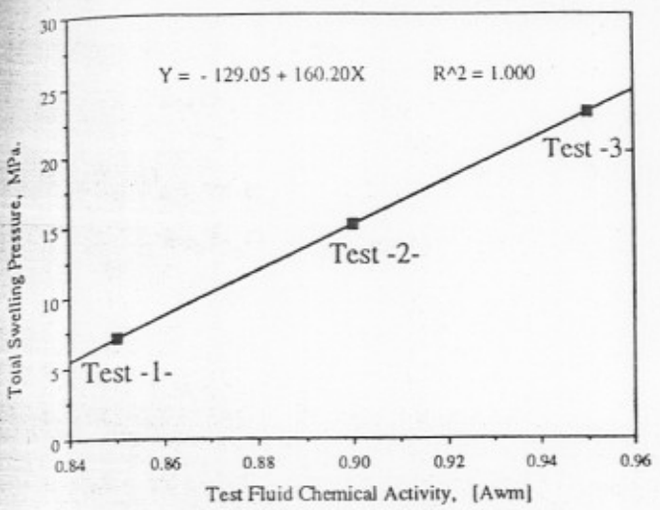

Fig. 16 : Relationship between 50 hours Experimental Total Swelling Pressure and Test Fluid Chemical Activity.

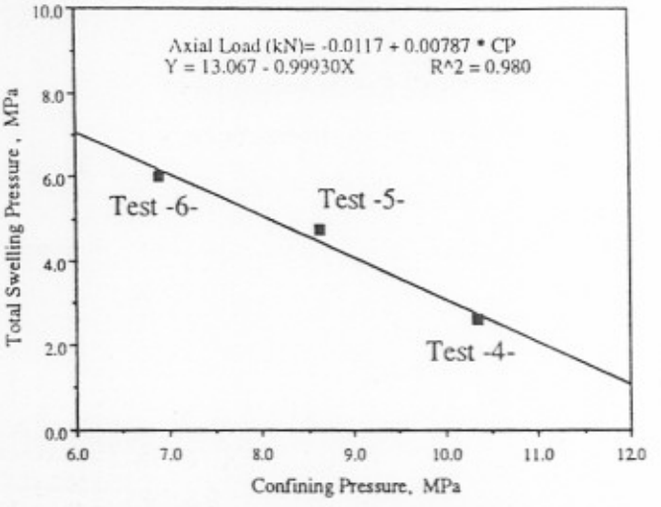

Fig. 17 : Relationship Between 52 hours Experimental Total Swelling Pressure and Confining Pressure.

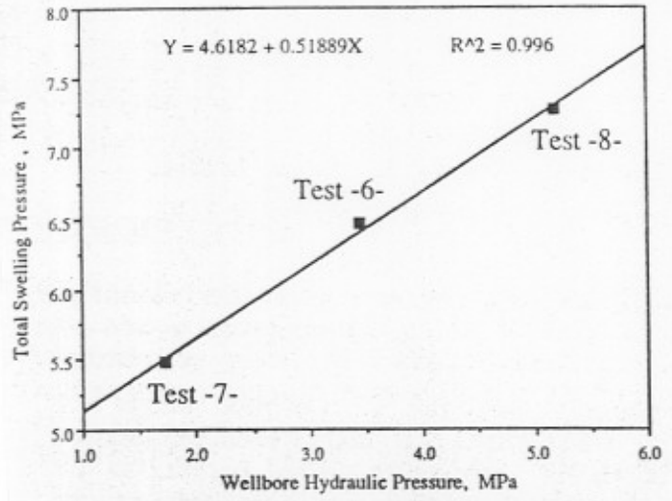

Fig. 18 : Relationship between 96 hours Experimental Total Swelling Pressure and Wellbore Hydraulic Pressure of FMS-Shale.

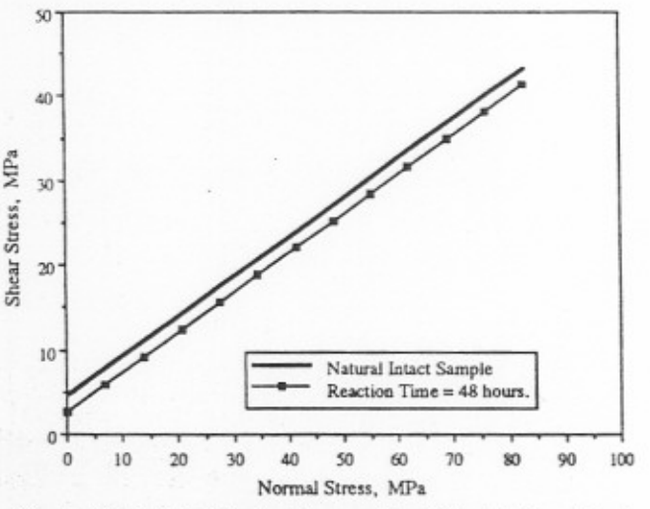

Fig. 19 : Effect of Total Swelling Stress on Mohr-Coulomb Failure Criterion Predicted based on Test -5- data on FMS-Shale.

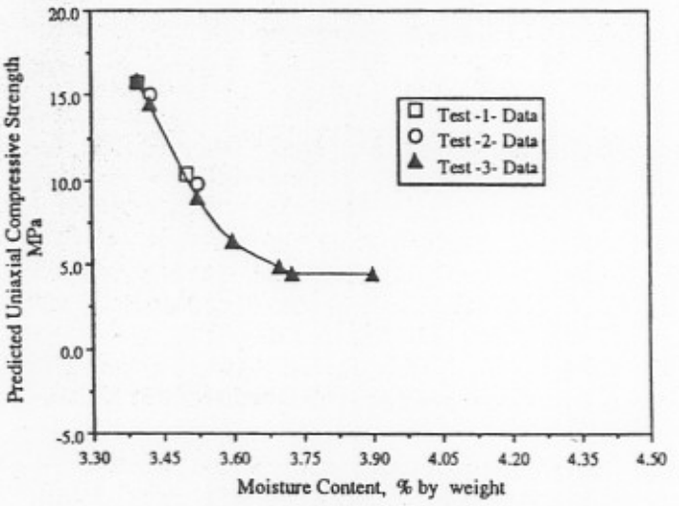

Fig. 20 : Relationship between Predicted Uniaxial Compressive Strength and Moisture Content for FMS-Shale.

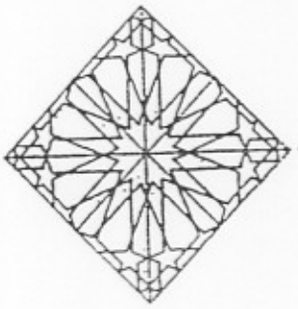

AEIC' 95

AL-AZHAR ENGINEERING FOURTH INTERNATIONAL CONFERENCE

December 16-19, 1995

FACULTY OF ENGINEERING
AL-AZHAR UNIVERSITY
Nasr City, Cairo, Egypt

VOLUME (10)
PETROLEUM ENGINEERING